Chemical Engineering Journal 283 (2016) 1522–1533

Contents lists available at ScienceDirect

Chemical Engineering Journal

journal homepage: www.elsevier.com/locate/cej

A comparative study on the adsorption of 8-amino-1-naphthol-3,6-disulfonic acid by a macroporous amination resin

Ziwei Zhang [a], Fang Wang [a], Weiben Yang [a,*], Zhen Yang [a], Aimin Li [b]

[a] School of Chemistry and Materials Science, Jiangsu Provincial Key Laboratory of Materials Cycling and Pollution Control, Nanjing Normal University, Nanjing 210023, PR China
[b] State Key Laboratory of Pollution Control and Resource Reuse, School of the Environment, Nanjing University, Nanjing 210046, PR China

HIGHLIGHTS

- A novel macroporous amination resin (GMDA) was employed to remove H-acid from water.
- GMDA owns advantage in the rapid adsorption equilibrium and high adsorption capacity.
- The reliable regeneration capacity of GMDA proves its practical applicability.
- The desired behaviors of GMDA is due to its suitable structural design.

GRAPHICAL ABSTRACT

The novel macroporous amination resin exhibits lower equilibrium time and better regeneration performance.

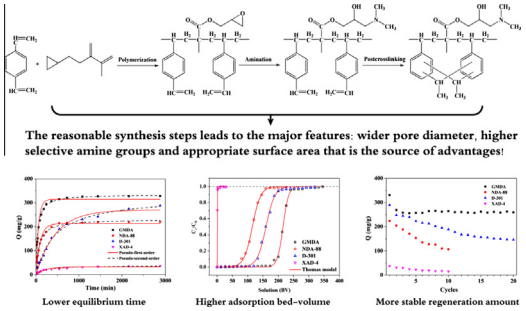

ARTICLE INFO

Article history:
Received 12 June 2015
Received in revised form 3 August 2015
Accepted 5 August 2015
Available online 18 August 2015

Keywords:
Amine resin
Regeneration circulation
Electrostatic interactions
8-Amino-1-naphthol-3,6-disulfonic acid
Adsorption

ABSTRACT

In this study, a novel macroporous amination resin (named as GMDA) with the matrix of divinylbenzene and glycidyl methacrylate was synthesized and utilized to remove 8-amino-1-naphthol-3,6-disulfonic acid (H-acid) from water. The adsorption behaviors of the synthetic resin were studied systematically and compared with three commercial resins (the hypercrosslinked resin NDA-88, the anion-exchange resin D-301, and the macroporous resin XAD-4) in terms of adsorption capacity, equilibrium time, isotherm adsorption, the effect of existing inorganic ions and regeneration properties. The characteristic methods of BET surface area, pore size distribution, SEM, FTIR, XPS and Zeta potential were investigated to analyze the resins and adsorption process. The GMDA resin has wider pore diameter than the NDA-88 resin to attract H-acid more quickly with higher adsorption amounts; the larger BET surface area of the GMDA resin ensures more binding sites than the D-301 resin in the adsorption process; the functional groups on the surface of the GMDA resin is more effective than the hydrophobic matrix of the resin XAD-4 in the removal of H-acid. Especially, the regeneration and dynamic experiments indicate the anti-fouling performance of GMDA resin is much better than the others. This research not only provides guidance for understanding the adsorption mechanism of H-acid onto the four resins, but also gives theoretical basis for the design of resin structure according to the targeted contaminants.

* Corresponding author.
E-mail address: yangwb007@njnu.edu.cn (W. Yang).

http://dx.doi.org/10.1016/j.cej.2015.08.010
1385-8947/

1. Introduction

8-Amino-1-naphthol-3,6-disulfonic acid (H-acid), one of the most typical naphthalene sulfonic organic compounds, has been widely used as an industrial intermediates. H-acid has been employed to synthetize various acidic, direct and reactive dyes because of its simple molecular structure in many factories [1]. However, the wastewater from the production process of H-acid with a lot of naphthalene sulfonic organic matters, inorganic salts and dark color, could not be treated thoroughly by the present wastewater treatment technology. This means that once in the water system, wastewater can cause negative impacts on the environment and human's health. In addition to the above mentioned harm, the price of H-acid in the market is seriously affected by the treatment of H-acid manufacturing process wastewater. These factories have to stop producing H-acid that will affect the local economic environment greatly, which can create a frustrating cycle. Therefore, it is important to find out a better treatment method for the wastewater from the manufacturing process of H-acid.

Many reports have displayed that the advanced oxidation technology was proverbially used to treat the industrial H-acid wastewater. Zhang et al. tried to use a microwave catalytic wet air oxidation of H-acid in aqueous solution under the atmospheric pressure using activated carbon as catalyst [2]. Liu et al. used the Fenton process to treat the wastewater, adjusted the relation of Fenton's reagent doses to reduce COD and TOC of the solution [3]. Noorjahan et al. degraded the molecular of H-acid onto a TiO_2 fixed bed reactor in the aqueous solution [4]. However, there is few literature about the adsorption of H-acid onto adsorbents, while the cost-effective adsorption technology for the industrial wastewater has been widely applied in many countries all over the world [5–9]. Previous researchers have made many efforts to deal with wastewater using various adsorbents, including resins, chitosan, and silica [10–13]. The adsorbents can be designed with binding sites with high selectivity and regenerated effectively, which could decrease the cost of the treatment and allow the process to be continuous. Due to the complex physicochemical properties of H-acid, authors had employed three commercial resins to adsorb H-acid from the aqueous solution, such as the hypercrosslinked resins (NDA-88), the anion-exchange resin (D-301) and the macroporous resin (XAD-4) [14–17]. Because of their unique advantages, they have been widely used in the wastewater treatment. However, the experimental results were not satisfactory because of their inevitable shortcomings that the possibility of engineering application was affected by their own limited characteristics: the mesopore and micropore of NDA-88 affects the continuous adsorption process; the smaller surface area of D-301 reduce the initial adsorption rate; the single hydrophobic interaction of XAD-4 is unable to reach the purpose of the adsorption of polar adsorbate onto the adsorbent. Therefore, authors expect to synthesize a novel resin that comprises the above advantages and avoids the disadvantages of the commercial resins.

In this research, based on the suspension polymerization technology for synthetic resins, a macroporous resin (GMDA) was synthesized and employed to remove H-acid in the aqueous solution. Taking the advantage in the adsorption of sulfonic groups onto amination resin into account, amine group was selected to modify resins [18–20]. The electrostatic attraction between H-acid and the resins defined the process of molecules accumulating from aqueous solution onto the exterior and interior surface of resins. The designed GMDA resin has the targeted functional groups, the wider pore diameter and the appropriate surface area. These characteristics would play an important role in the process of adsorption and regeneration adsorption–desorption cycles. Various characteristic analysis method of the scanning electron microscope (SEM), the Zeta potential, the Fourier transform infrared spectroscopy (FTIR) and the X-ray photoelectron spectroscopy (XPS) were used to explain the adsorption experiment and mechanism. Improving the adsorption performance, simplifying synthetic process of resins and reducing the environmental pollution of wastewater containing H-acid are the main goals of this research. Moreover, effects of pH, time, temperature and inorganic anions were systematically investigated.

2. Materials and methods

2.1. Materials

8-Amino-1-naphthol-3,6-disulfonic acid monosodium salt was obtained from Aladdin Industrial Inc., China. The molecular structures and selected physicochemical properties of H-acid were shown in Fig. 1. Divinylbenzene (DVB, 80%), glycidyl methacrylate (GM, 97%), dimethylamine (DA, 40%), trimethylamine (TA, 33%), diethylamine (DE, 99.0%), ethanol and methanol were purchased from Aladdin Industrial Inc., China. Benzoyl peroxide (BPO), 2,2-azobis (AIBN), $FeCl_3$, 1,2-dichloroethane, gelatin, toluene, $NaNO_3$, NaCl, Na_2SO_4, Na_3PO_4, Na_2HPO_4 and NaOH were purchased from Sinopharm Chemical Reagent Co., Ltd.

2.2. Preparation of adsorbents

Commercially available resin D-301 and XAD-4 were supplied by the Shanghai Office, Purolite International Co., Ltd. Hypercrosslinked polymeric adsorbent resin NDA-88 was obtained from Nanjing University.

The GMA resin was synthesized through a suspension polymerization process with 12.5 g of GM and 12.5 g of DVB as monomers and 25.0 g of toluene as porogen in a glass flask with 1 g BPO and 1 g AIBN as the initiator. 2 g gelatin, 1.05 g Na_3PO_4, 4.2 g Na_2HPO_4, 32 g NaCl and 200 mL deionized water employed as the dispersion phase. The mixture was stirred in the 500 mL flask at 368 K for 12 h. Resins were collected and rinsed with deionized water at 343 K and then washed by methanol to remove the unreacted monomers and porogen. The resins were vacuum dried at 333 K for about 12 h. After drying, the microspheres were modified with the different volumes of DA/TA/DE solution at 338 K for 12 h to introduce amine groups, respectively. After washing with deionized water several times the effluent was neutral, all of the ammonium groups microspheres were cross-linked by reaction with 1,2-dichloroethane and $FeCl_3$ at 353 K for 24 h. The resin was rinsed repeatedly with methanol and HCl until the effluent was clarified, then washed with deionized water to neutral and dried at 333 K for 12 h.

Before the conventional experiments, the better substitution degree had been investigated; the series of resins were synthesized with the different dosage of 5 mol/L DA/TA/DE and the resin GMA.

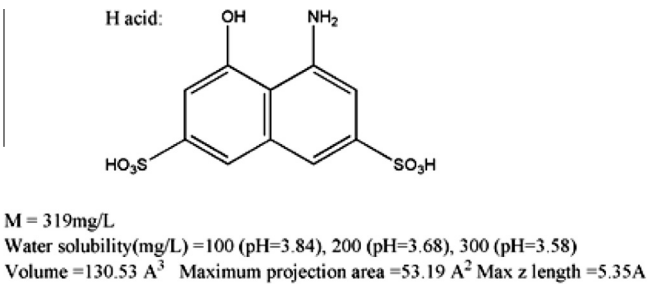

Fig. 1. The molecular structure and physicochemical properties of H-acid.

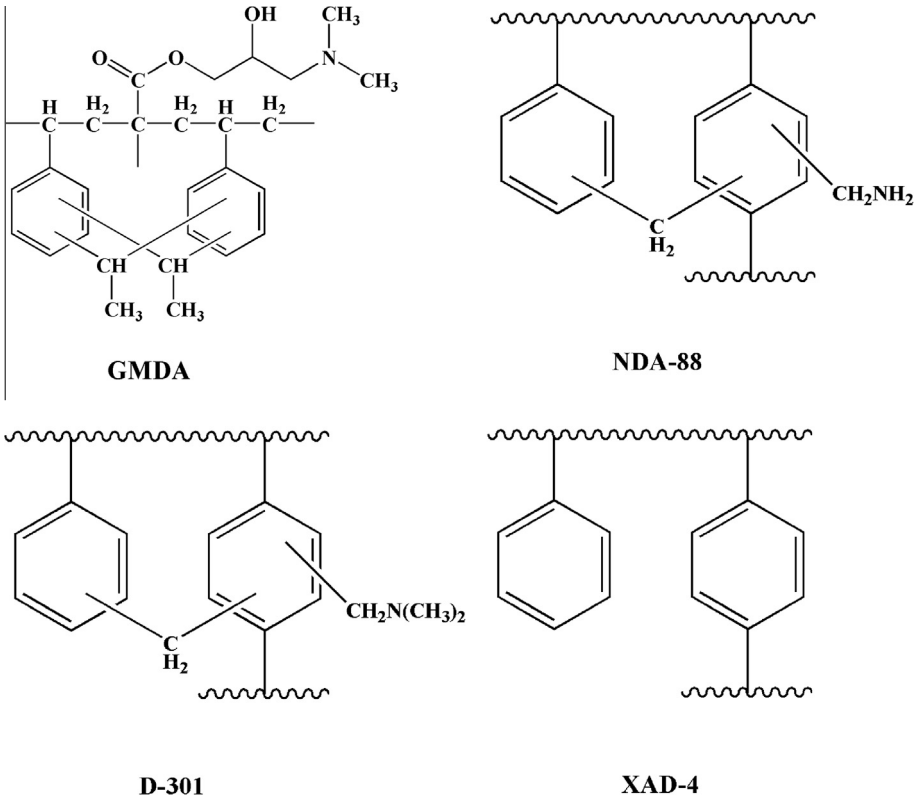

Fig. 2. The structure of the GMDA resin and three commercial resins: NDA-88, D-301 and XAD-4.

20 g resin GMA was modified with 25 mL, 75 mL, 150 mL and 250 mL of 5 mol/L DA/TA/DE solution. The exchange capacities and adsorption amounts were measured (Table S1), and then the resin with the maximum adsorption capacity was selected and named as GMDA. The structures of the resin GMDA and commercial resins were shown in Fig. 2.

2.3. Instrument analysis

The exchange capacity of the synthetic resin was determined by the Chinese measurement standard (GB/T 5760-1986, Method for the determination of exchange capacity of anion exchange resin). The resins and H-acid solution were thoroughly mixed and the flasks were completely sealed and placed in the incubator shaker (New Brunswick, Model G25) at the specific temperatures. The aqueous samples were taken out at preset time intervals to determine the remaining concentrations of the adsorbates. A Perkin–Elmer 240C Elemental Analytical Instrument (Wellesley, MA, USA) was used to perform the elemental analysis of four resins. Fourier transform infrared (FTIR) spectra before H-acid adsorption were recorded using a Nicolet 170 IR spectrometer (Madison, WI, USA) at ambient temperature. An automatic analyzer (Micromeritics ASAP-2010C, USA) was used to determine the BET surface area and pore diameter of resins with N_2 as the adsorbent. The pH values were tested with a pH meter (Thermo 520M-1, USA). Zeta potential and X-ray photoelectron spectroscopy (XPS) were measured by a Malvern Nano-Z Zetasizer and a ULVAC-PHI 5000 VersaProbe XPS spectrometer, respectively. 0.05 g of resin was milled into powder and added into 100 mL deionized water to shake uniformly, than adjust pH to measure potentials. The morphology of resins was investigated by SEM images, which was obtained from a field emission SEM (ZEISS, Germany). Before measured, all of the samples were freeze-dried prior.

2.4. Adsorption assay

The synthetic resin with amine groups was used in this adsorption study. For the adsorption kinetics, four 1000 mL flasks with 500 mL of 200 mg/L H-acid aqueous solution were shaken respectively with 0.250 g selected resins under constant stirring with a shaking speed of 140 r/min. The adsorption equilibrium experiments were performed at 303 K for 48 h. Meanwhile, 0.05 g resin was introduced to each 150 mL conical flasks. 100 mL of H-acid aqueous solution were then added to each flask and the initial concentrations of the solution were 100, 150, 200, 250 and 300 mg/L, respectively. The pH of solution was adjusted to 2–8 using 1 mol/L HCl or 0.1 mol/L NaOH solution, respectively. 0.01–0.1 mol/L NaCl, Na_2SO_4 and $NaNO_3$ was added separately in the H-acid aqueous solution to study the effect of ions strength on adsorption capacities. At last, the flasks were completely sealed and placed in the shaker at 288, 303 and 318 K for 48 h. The concentrations of adsorbate in the solutions were obtained by measuring the UV adsorption at 235 nm for H-acid (UV analyzer, Mapada UV3100-PC, China) [21]. Adsorption data were collected for all the above experiments. The adsorption amount, q_e (mg/g), was calculated using Eq. (1):

$$q_e = \frac{V(C_0 - C_e)}{m} \quad (1)$$

where C_0 and C_e are the initial H-acid concentration (mg/L) and the concentration at equilibrium (mg/L), respectively. V is the volume of solution (L), and m is the weight of the dry adsorbent (g). All adsorption experiments were repeated three times. The error rate of the adsorption capacity was less than 3%.

2.5. Regeneration and dynamic adsorption

In order to study the practical application of the resins, adsorption regeneration and continuous column-mode experiments were

carried out. 100 mL of 200 mg/L H-acid solution and 0.050 g resin were shaken at 303 K until the adsorption equilibrium was reached. The GMDA resin was desorbed by various mixed desorption solution at 303 K. After the desorption equilibrium, the solution concentration of H-acid was determined by UV measurements. The better desorption solution was chosen to desorb the GMDA resin in the regeneration experiments. For dynamic adsorption, a complete system of a glass column (10.0 mm in diameter and 100 mm in length) with water baths to the temperature stable in 303 K that experiment picked up with GMDA, NDA-88, D-301 and XAD-4 for the aqueous solution containing H-acid. The initial concentration of H-acid is 1000 mg/L, and the initial pH is 2.96. The flow rate was 4 BV/h (1 BV = 7.85 cm^3, that was the volume of adsorption column).

3. Results and discussion

3.1. Characterization of resins

The adsorption amount is an important parameter to evaluate the resin. The effects of the molar ratio of DA/TA/DE and GMA on the adsorption of H-acid onto resin was firstly evaluated. The exchange capacities of these resins were characterized in Table S1 in Supporting information. The scheme of preparation was exhibited in Fig. S1 in Supporting information, then named as GMDA and used in the following experiments.

3.1.1. FTIR

FTIR is a useful tool to identify the presence of certain functional groups of adsorbents. In this study, the changes of groups on the resins are found by FTIR analysis. FTIR of resin GMA and GMDA (Fig. 3) are complex due to the presences of different functional groups on the surfaces of these two resins. Among the FTIR spectra of two synthetic resins, the main peaks at 1732 (C=O stretching), 1609 (ester groups), 1473 (C—H), 1347 (CH_3 from methacrylate structure), 997 (C=C), 910 (epoxy groups) and 711 cm^{-1} (benzene) mean that the GMA resin was synthesized successfully. In the spectra of GMDA, the peak occurred a displacement from 1201 to 1276 cm^{-1} obviously, indicating C—N was introduced into the resins. Thus, GMDA resin was confirmed to be synthesized successfully. Similarly, the FTIR spectra of NDA-88 and D-301 indicate the presence of amine functional groups in 2779 and 1270 cm^{-1}, respectively. The carbonyl and hydroxyl groups are detected on the surface of NDA-88 relating to its hypercrosslinked structure.

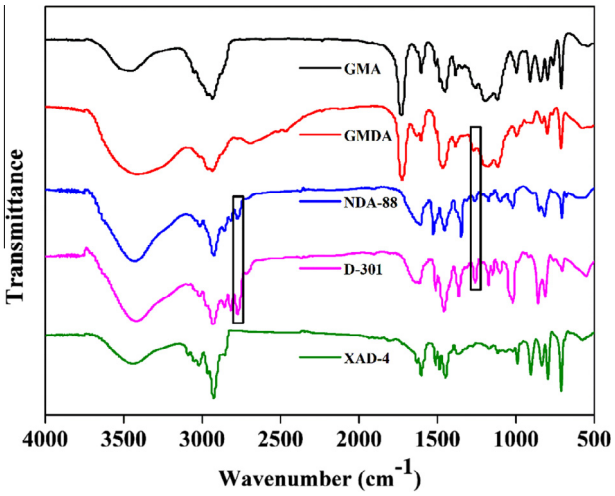

Fig. 3. FTIR spectra of GMA, GMDA, NDA-88, D-301 and XAD-4.

3.1.2. Selected characteristics

The physicochemical properties of the four selected resins and the adsorption capacity of H-acid onto resins are presented in Table 1. Although the BET surface area of the macroporous resin XAD-4 is the larger than the resin GMDA that would provide more active region for adsorption theoretically, the adsorption capacity of H-acid onto XAD-4 is minimum, which means the hydrophobic interaction is not the main contributor to the adsorption of H-acid. The smaller BET surface area of GMDA should result from the larger average pore diameter. Interestingly, the GMDA resin has the maximum adsorption capacity among the four resins as listed. The presence of a relatively great mount of nitrogen (2.90%) on the surface of GMDA mean that the existence of tertiary amine functional groups. Moreover, the anion-exchange resin D-301 also presents the removal of H-acid. Resin D-301 is composed of styrene divinylbenzene copolymer, then is modified by tertiary amine groups and possesses anion-exchange mechanism. Due to the minimum surface area, the nitrogen (2.43%) from amine functional groups is gathered on the surface of resin D-301. H-acid will be mainly adsorbed on the surface of D-301 rather than diffuse into the internal pore of resins. The adsorption capacity and rapid adsorption speed of D-301 may be influenced by the above characteristics. This should be attributed to the interaction between the amine groups on the resins and the sulfonic groups of adsorbate H-acid. Although NDA-88 contains rich amino groups on its surface, its micropores apparently restrict adsorption diffusion and interaction. These specific disadvantages will be further discussed in the next step.

3.1.3. Pore structure

The pore size distributions of the four resins are shown in Fig. 4. The pore size distributions of GMDA and D-301 is similar to that of XAD-4: The macropore and mesopores in the range of 5–17 nm dominate the pore of GMDA and no obvious micropores are observed; the pore diameter distribution of NDA-88 resins is in a narrower micropore region (1–2 nm) and a large amounts of micropores are emerged. The micropore structure of NDA-88 should result in its lower adsorption amount as H-acid molecules are likely to congregate at the micropore entrance after the initial rapid adsorption process. Although the approximate pore structure, the BET surface area of D-301 is much less than that of GMDA, which would affect the available groups, exposed in the internal pore of the resin D-301 and GMDA. So dense amine group precipitate the strong molecular affinity on the surface of D-301 that makes two possible disadvantages, the easily blocked pore by H-acid molecules, and the lower desorption efficiency [22,23]. The resin GMDA can be treated as the special resin with amine group, wider pore diameter and cross-linked properties, the comprehensive characteristics contribute to the advantage in initial rapid adsorption process and regeneration adsorption in the following study.

3.2. Effect of pH on the adsorption

As one of the most important characteristic methods for adsorption mechanism, Zeta potentials (ZPs)–pH profiles of four resins and H-acid were measured and illustrated in Fig. 5(A). Considering the pH of wastewater containing H-acid is usually lower than 7, ZPs was investigated within the pH of 2–8. The resins GMDA, NDA-88 and D-301 with amine groups exhibit the positive charge with protonation appearance in the acid environment while the XAD-4 presents corresponding isoelectric points due to the non-functional group structure. So, large amounts of free-state sulfonic acid groups make the charge of H-acid below the isoelectric point, which causes a strong charge interaction with the resins of amine group [24]. According to the Zeta potential–pH profiles, the best

Table 1
The BET data and selected characteristics of synthetic resins and three commercial resins.

Properties	GMDA	NDA-88	D-301	XAD-4
The adsorption amount of H-acid onto the resins, mg/g	327.91	220.93	288.10	35.94
Main functional groups	$-N(CH_3)_2$	$-NH_2$	$-N(CH_3)_2$	–
BET surface area, $m^2\ g^{-1}$	218.13	531.12	38.20	898.63
Micropore area, $m^2\ g^{-1}$	14.97	278.01	9.03	223.36
Average pore diameter, nm	11.3	1.20	8.94	5.61
Nitrogen, % (wt/t)	2.90	1.98	2.43	–
Particle size, mm	0.3–0.5	0.3–0.5	0.3–0.5	0.3–0.5

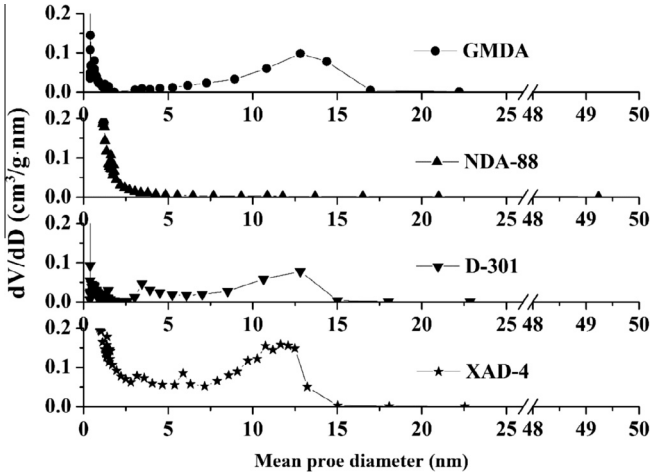

Fig. 4. The pore diameter distribution of GMDA, NDA-88, D-301 and XAD-4.

adsorption performances might occur within the pH 2–4 due to the electrostatic interaction. Moreover, the adsorption performance would be weakened with the increasing pH value. Hence, the adsorption experiments were carried out within the above pH range.

As shown in Fig. 5(B), the adsorption capacity of H-acid onto the resins at different pH values was different with each other. The adsorption capacity of the four reins as follows: GMDA > D-301 > NDA-88 > XAD-4.

At the common pH value, the greater adsorption capacity of resin GMDA and D-301 in contrast with the resin NDA-88 indicates that the tertiary ammonium group has a more positive effect on the adsorption of H-acid than amino groups of NDA-88 [15]. When pH is in the range of 3–4, the adsorption amounts stay at the highest level. Adsorption amount is minimum when pH is 2. The presence of 0.01 mol/L chloride ions could be the main influencing factors, and competitive adsorption occurs between H-acid and chloride ion. This adsorption phenomenon will be confirmed in the following discussion of coexisting ions. On the other hand, a small amount of sulfonate groups takes off the protons in the condition of lower pH value, and the amine group forms quaternary at the same time. With the pH increasing, a large of number of sulfonate groups are deprotonated. Therefore, the adsorption capacities obviously decrease when pH increase to 8 that validates our previous inference in the analysis of ZPs. Interestingly, the pH of aqueous solution containing 100–300 mg/L of H-acid is within 3.84–3.58, which is within the best region to the adsorption of H-acid onto the GMDA and commercial resins. Similarly, this pH range will be employed in the following discussion.

3.3. Adsorption kinetics

Adsorption kinetics is very important in the characterization and study of the efficiency and feasibility of the resins on the practical application. The adsorption kinetics of the four resins in the aqueous solution containing 200 mg/L of H-acid were studied. The data is displayed in Fig. 6. It can be clearly seen from the parameters that the rate constants for adsorption of H-acid onto all the adsorbents change in the same order with the maximum adsorption capacity: GMDA > D-301 > NDA-88 > XAD-4, indicating that the adsorbate molecules was adsorbed more faster in the wider pore region of resin with larger adsorption capacity. The affinity of adsorbate onto adsorbent depends on the interactions between the surface of the adsorbent and the structure of the molecule by π–π interactions, hydrophobic interaction, electrostatic interactions and so on. Molecules containing different physical properties could interact in many ways with an adsorbent and the liquid phase. In terms of the acrylic matrix of the resins, π–π interactions should be less important because such interactions

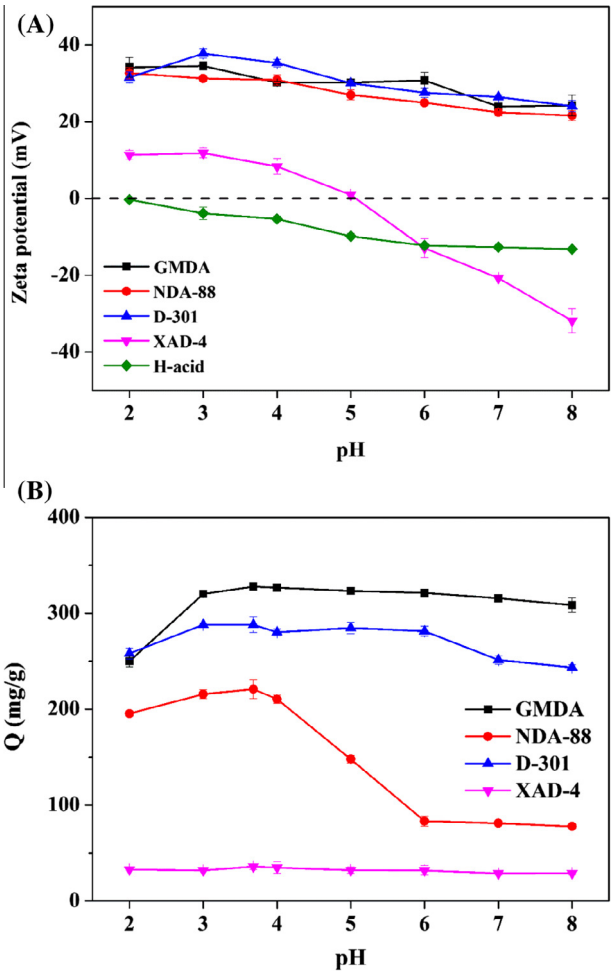

Fig. 5. (A) Zeta potential–pH profiles and (B) the effect of pH on the adsorption capacities of 200 mg/L H-acid onto four resin at 303 K.

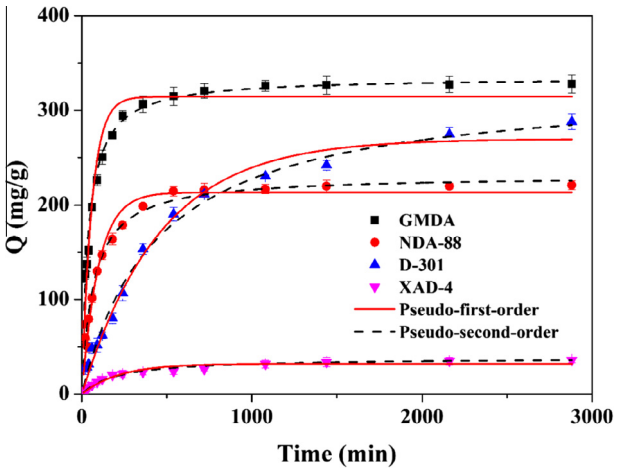

Fig. 6. The adsorption kinetics of H-acid onto four resins at 303 K, the initial concentration of H-acid aqueous solution is 200 mg/L.

are restricted to aromatic rings. The presence of sulfonate groups of H-acid results in a negative charge on molecules under both acidic and basic conditions appears anion-exchange with tertiary amine resins positively charged [25]. As shown in Fig. 6, the adsorption capacity of H-acid onto the resin XAD-4 is far less than the adsorption amount onto the resin GMDA. The adsorption amounts of the resin XAD-4 should originate from less contribution of hydrophobic interaction in this process. The electrostatic interaction between amine group and H-acid displays the significant role. The adsorption of H-acid onto the resin GMDA demonstrated relatively fast speed and rapid adsorption occurred within the first 90 min. In fact, for the resin GMDA, with amine groups and macroporous matrix, adsorption can be believed to occur mainly in the macroporous region. For four resins listed in this work, the effect of the mesopore and micropore region can be negligible in H-acid adsorption, and the higher surface area of GMDA than D-301 doesn't play a positive role legitimately. This phenomenon also confirms our speculation that the adsorption performance of adsorbent is constrained by structure characteristic consisting of the surface area, pore diameter, effective functional group and so on. The adsorption capacity onto the resin D-301 is close to the resin GMDA, but the D-301 consumes longer time to reach adsorption equilibrium. The smaller BET surface area and pore diameter seem to be the major factors. Although the adsorption efficiency of H-acid onto the resin NDA-88 is similar to GMDA, its mesopore and micropore hinder the diffusion of more molecules into resin surface when a great number of molecules are adsorbed on the pore entrance. Comparing with pore diameter of GMDA, macropore could ensure the molecules of H-acid continuously entering into the resin.

To analyze the kinetics of adsorption further, the pseudo-first-order model and pseudo-second-order model were used to confirm the H-acid adsorption onto the four resins. The equations are listed as follows:

$$\text{Pseudo-first-order}: Q_t = Q_e(1 - \exp(-k_1 t)) \quad (2)$$

$$\text{Pseudo-second-order}: Q_t = \frac{k_2 t Q_e^2}{1 + k_2 t Q_e} \quad (3)$$

where Q_e (mg/g) is the capacity of resins adsorbed H-acid at equilibrium time, and Q_t (mg/g) is the capacity of resins adsorbed H-acid at time t. k_1 (min^{-1}) and k_2 (g/mg·min) are the pseudo-first-order model and pseudo-second-order model rate constants, respectively. The fitting data were listed in Table 2. The pseudo-second-order model better described the adsorption behavior of H-acid onto the resin GMDA, and certifying the effect between resin and H-acid being chemical adsorption [26,27]. The value of the constant of k_2 for H-acid adsorption onto GMDA (0.0079×10^{-4} g/mg·min) is obviously greater than those onto NDA-88 (0.0006×10^{-4} g/mg·min) and D-301 (0.0007×10^{-4} g/mg·min), which may directly relate to the adsorption rate. The H-acid molecules may be able to easily diffuse in the macropore surface than enter the mesopore area, even wedge into the smaller micropores. Therefore, the diffusion of H-acid within the resin NDA-88 is slower as the adsorption rate listed, the equilibrium time for NDA-88 are greater than GMDA. The difference of k_2 between the resin GMDA and D-301 was studied, and the cause of this difference was not similar to the different diffusion between NDA-88 and GMDA. H-acid molecules will get more opportunities to be adsorbed by the ordered amine group on the surface of the resin GMDA, which has greater surface area than D-301. In contrast, D-301 has concentrated, intensive amine groups in the smaller surface, thus hindering rapid molecule diffusion in the exterior and interior surface of D-301 equably. A conclusion can be summarized that the amine groups, wider pore diameter and proper surface area are important factors in the H-acid adsorption process. There interesting findings are also consistent with the goal of this work [18].

3.4. Adsorption isotherm and thermodynamics

The adsorption isotherms of H-acid onto the GMDA and commercial resins at different temperatures are depicted in Fig. 7. As hydrophobic interaction didn't play a major role, the adsorption capacity of H-acid onto XAD-4 was weaker than the other three resins. It can be seen that the equilibrium adsorption amounts of H-acid onto the same resin have a small increase with the increase of temperature. This means the higher temperatures intensify molecular motion and expand the channels in the interior of resins. The similar characteristics of adsorption behavior might result from the same adsorption mechanism between the adsorbent and adsorbate.

The Langmuir and Freundlich isotherms are two typical isotherms for describing the adsorption on adsorbents from aqueous solutions. To further assess the significance of the resin properties in the adsorption process of H-acid, Langmuir isotherms (Eq. (4)) and Freundlich isotherms (Eq. (5)) models were used to fit the experiment data.

$$Q_e = \frac{Q_m K_L C_e}{1 + K_L C_e} \quad (4)$$

$$Q_e = K_F C_e^{1/n} \quad (5)$$

Table 2
The kinetic data for the adsorption of H-acid onto four resins.

Resins	Pseudo-first-order model			Pseudo-second-order model		
	Q_e (mg/g)	$k_1/10^{-2}$ (min^{-1})	R^2	Q_e (mg/g)	$k_2/10^{-2}$ (g/mg·min)	R^2
GMDA	314.43	1.723	0.896	335.07	0.0079	0.980
NDA-88	213.31	1.028	0.929	231.15	0.0006	0.954
D-301	269.81	0.218	0.984	328.03	0.0007	0.990
XAD-4	32.12	0.461	0.949	36.77	0.0148	0.983

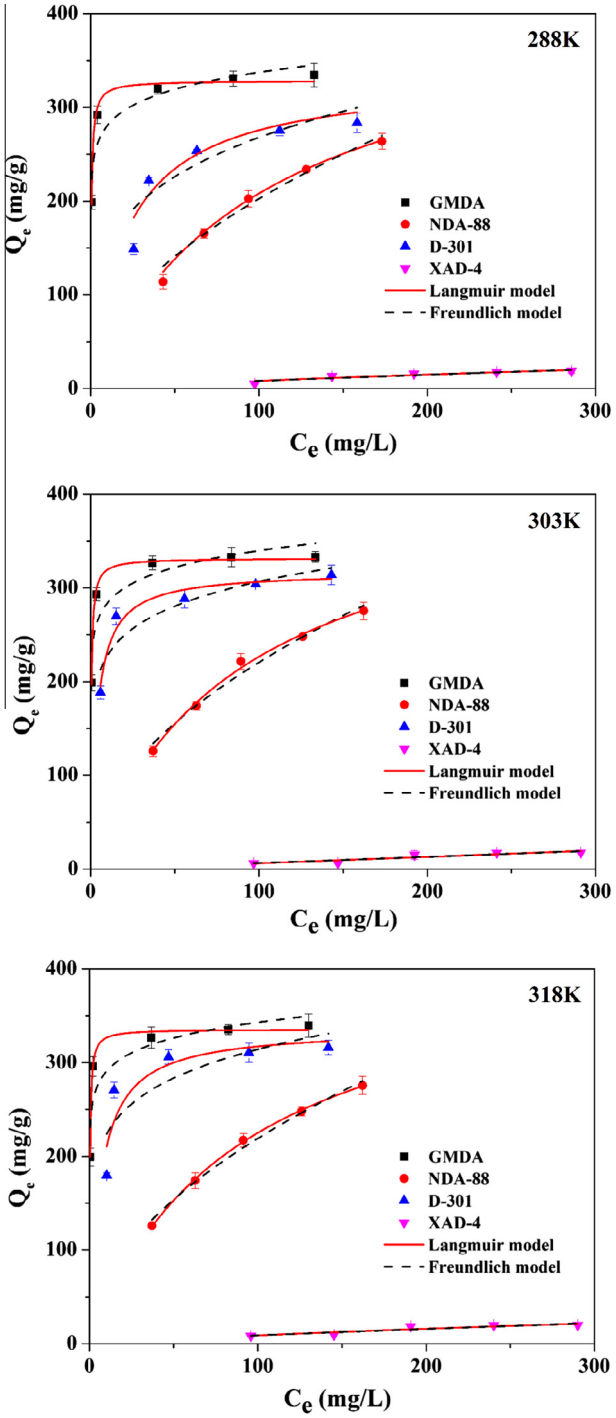

Fig. 7. The adsorption isotherms of H-acid onto resins at the different temperatures: 288, 303 and 318 K.

where Q_e (mg/g) and C_e (mg/g) are the adsorbate concentration and the concentration of H-acid aqueous solution at adsorption equilibrium, respectively, and Q_m (mg/g) and K_L (L/mg) represent the maximum adsorption amount and the affinity of the binding sites, respectively. K_F (L/g) and n are the Freundlich adsorption parameters, which indicate adsorption amount and intensity, respectively. According to Table 3, the Langmuir model provides a better match for model most of the experimental parameters than the Freundlich model for GMDA according to R^2 value. The Langmuir model assumes that resins have a limited number of adsorption sites in the ideal condition. This adsorption model could be described as the monolayer adsorption. Electrostatic attraction between sulfonic group and functional groups make the adsorption process occurred rapidly. When the temperature increases, the adsorption capacity of the above adsorbents increases a little, which is the special characteristic of electrostatic interaction without a great change with temperature. With the concentration increasing, the surface and internal of adsorbent become saturated when maximum concentration is reached. Moreover, some other obvious information could be known from the fitting data. According to the $1/n$ value ($1/n < 0.1$), H-acid is adsorbed onto the resin GMDA easily [28]. The anion-exchange mechanism and electrostatic interactions are essential to the adsorption behavior of H-acid onto the resin GMDA. The commercial resins don't show such strong affinity. This phenomenon confirms the applicability of the resin GMDA in industrial wastewater treatment.

To describe the thermodynamic behavior of adsorption of H-acid onto four resins, the thermodynamic parameters of the adsorption process can be calculated as free energy (ΔG), enthalpy change (ΔH), and entropy change (ΔS). Free energy of sorption was calculated with use of equation:

$$\Delta G = -RT \ln K_L \tag{6}$$

where R is the gas constant (8.314 J/(mol * K)) and T is temperature (K). The partition coefficient K_L (dm^3/mg) varied with change of temperature. K_L parameter was calculated by plotting C_e/q_e versus C_e (Langmuir mathematical model).

$$\ln K_L = \frac{\Delta S}{R} - \frac{\Delta H}{RT} \tag{7}$$

where ΔH (kJ/mol) and ΔS (J/(mol * K)) were calculated from the slope and intercept of $\ln K_L$ versus $1/T$ plot. The thermodynamic parameters for the adsorption of H-acid onto four resins at various temperatures are enumerated in Table 4. The negative ΔG value indicate that the adsorption of H-acid onto GMDA, NDA-88 and D-301 is spontaneous at 288, 303 and 318 K. The positive ΔH suggests that the adsorption reaction is endothermic surface reaction [29–31]. However, the adsorption capacity of H-acid increased a little with the increased temperature that may be affected by the principle of expansion and contraction and kinetic molecular theory. The ΔS is positive, which indicates that the increased randomness at the solid-solution interface during the adsorption of H-acid onto three resins [32]. For XAD-4, ΔS of the process is negative, and upon reaction is a decrease of randomness at the solid–liquid interface.

3.5. Effect of the coexisting ions

Effect of the coexisting ions on adsorption capacity of H-acid onto resins was displayed in Fig. 8. In many previous studies, cations have no discernible effect on the adsorption process of substances with negative charges onto anion exchange resins [17]. Previous publications show that the effects of anions on contaminants removal by tertiary ammonium resin is different [33,34]. Due to the existence of different ions concentration and species, the adsorption capacities decreased in the order: $SO_4^{2-} > NO_3^- > Cl^-$. The existence of anions impedes the exchange of the adsorbates with the resins, then a competitive adsorption may occur [35,36]. More sites are combined with more inorganic ions and spare amine groups are less. This evidence could be applied in the regeneration adsorption process. With the further analysis of twice dissociation, a characteristic was observed that more amine groups are occupied by sulfate ion with two negative charges than Cl^- with only one negative charge under the equal concentration and the amount of charges plays an important role in this comparative test. The previous studies reported various resins with amine groups had high efficiency adsorption behavior of inorganic anions [37,38]. The increasing electrostatic interactions between the negatively

Table 3
The adsorption isotherm model constants for the adsorption of H-acid onto four resins at 288, 303 and 318 K.

Resin	T (K)	Langmuir model			Freundlich model		
		K_L (L/mg)	Q_m (mg/g)	R^2	K_F (L/g)	n	R^2
GMDA	288	2.631	326.76	0.992	234.03	12.832	0.805
	303	2.586	331.70	0.996	237.49	12.863	0.777
	318	3.556	335.52	0.993	246.21	13.892	0.751
NDA-88	288	0.010	422.52	0.956	18.327	1.917	0.904
	303	0.011	424.43	0.994	21.690	1.986	0.974
	318	0.011	426.99	0.999	20.915	1.96	0.987
D-301	288	0.048	334.57	0.744	87.020	4.095	0.590
	303	0.274	335.05	0.964	169.513	7.764	0.799
	318	0.163	336.61	0.772	158.77	6.749	0.588
XAD-4	288	0.001	62.357	0.801	0.200	1.236	0.776
	303	0.001	78.031	0.880	0.20	0.999	0.657
	318	0.001	78.169	0.789	0.24	1.298	0.853

Table 4
Values of thermodynamic parameters evaluated for H-acid adsorption onto four resins.

Resin	T (K)	ΔH (kJ/mol)	ΔS (J/(mol * K))	ΔG (kJ/mol)
GMDA	288	18.07	7.31	−2.09
	303	18.86	7.59	−2.28
	318	22.32	7.81	−2.46
NDA-88	288	10.76	13.01	−3.74
	303	11.30	13.14	−3.97
	318	11.82	13.31	−4.22
D-301	288	11.82	7.73	−2.21
	303	13.00	7.76	−2.34
	318	13.33	7.84	−2.48
XAD-4	288	13.40	−12.10	3.50
	303	14.02	−9.99	3.04
	318	14.71	−9.97	3.19

charged ions and positively charged amine groups cause an increase in the anions adsorption. Therefore, the general trend is obtained that anion concentration has a negative effect on the H-acid removal by anion-exchange mechanism [39].

3.6. Characterization after adsorption

As the speculation we presented through the structure analysis, the adsorption can also be observed by the scanning electron microscope (SEM) on the surface of the samples in Fig. S2 in Supporting information. Fig. S2(A–D) mainly reveal the macropore structure of GMDA, the micropore region of NDA-88, the meso/-macropore structure of D-301 and XAD-4 before the adsorption, respectively. As shown in Fig. S2(E–H), the resins' surface present different adsorption state, except for XAD-4, which shows no significant adsorption. From the Fig. S2(E), a large amount of H-acid molecules focus on the surface, and a part of the duct is not blocked completely that means GMDA keeps the adsorption until the adsorption equilibrium was stayed. Contrarily, compared with Fig. S2(B and C), the H-acid on the surface of NDA-88 and D-301 in Fig. S2(F and G) that sheet successfully covered on the surface. Most of the holes are hidden so that there are no obvious pore observed on exterior of two resins [40–42]. By electron microscopy observation above, the macropore structure of GMDA is very ideal.

The FTIR spectra of the four resins before and after adsorption is shown in Fig. S3 in Supporting information. A conclusion could be drawn that H-acid is adsorbed by GMDA, NDA-88 and D-301: The special peaks at 1192, 1195 and 1189 cm^{-1} (S═O from sulfonic acid group of H-acid) and the peaks at 675, 674 and 673 cm^{-1} (S—C stretching) are revealed in the spectra of three resins after adsorption. However, there are no obvious S═O and S—C stretching peak detected in the spectra that should be caused by the very low adsorption capacity.

XPS characterization of the resins was performed to further investigate the change of chemical structure before and after adsorption. Fig. 9 shows the survey data, indicating that the above resins contain two element N and S. The XPS spectrum of N1s and S2p of GMDA is shown in Fig. 9(a), which can be analyzed as two peaks of free tertiary amine group and protonated tertiary amine group centered at 398.55 and 401.38 eV, respectively. Although washed by deionized water until the effluent was neutral, HCl protonated free tertiary amine group, and neutral environment can't make all the tertiary amines to deprotonation effect. After H-acid was adsorbed by GMDA, the peak of protonated tertiary amine groups shifted to higher peak with stronger intensity, and a new peak was detected in 398.46 eV. Amino group signals may be covered with protonated tertiary amine group, and then the stronger peak emerged. Moreover, with the adsorbed H-acid, the peak position is enhanced towards the original peak signal in N1s (GMDA). The only N1s spectrum is revealed in N1s (NDA-88) of Fig. 9(b), then two peaks centered at 398.46 and 401.4 eV are shown after adsorption. However, as shown in Fig. 9(c), a weak peak at 401.04 eV means the protonated tertiary amine group on the surface of D-301, although tertiary amine group is the major functional group on its surface. In terms of the adsorption of GMDA, the stronger peak at 401.15 eV illustrates superimposed of protonated tertiary amine group and the amino group of H-acid [43].

All S2p spectra of four resins before adsorption were not deconvoluted to any peaks. Nevertheless, after adsorption, the S2p spectra of GMDA, NDA-88 and D-301 were revealed at the increased peak of 167.28, 166.98 and 166.76 eV, respectively. This illustrates that H-acid was adsorbed on the surface of the above resins [43]. In Fig. 9(d), no peak is shown in the N1s and S2p spectra of XAD-4 before and after adsorption that attributes to the chemical structure of XAD-4 without any amine functional group and much less adsorption capacity.

To sum up, FTIR and XPS analysis were employed, showing that the H-acid molecule was adsorbed on the surface of resins. The parameter at special peaks can be described as our speculation from the experimental phenomenon.

3.7. Regeneration and column-mode experiment

From the above experiment phenomenon, the resin GMDA has been successfully applied in the removal of H-acid in various exper-

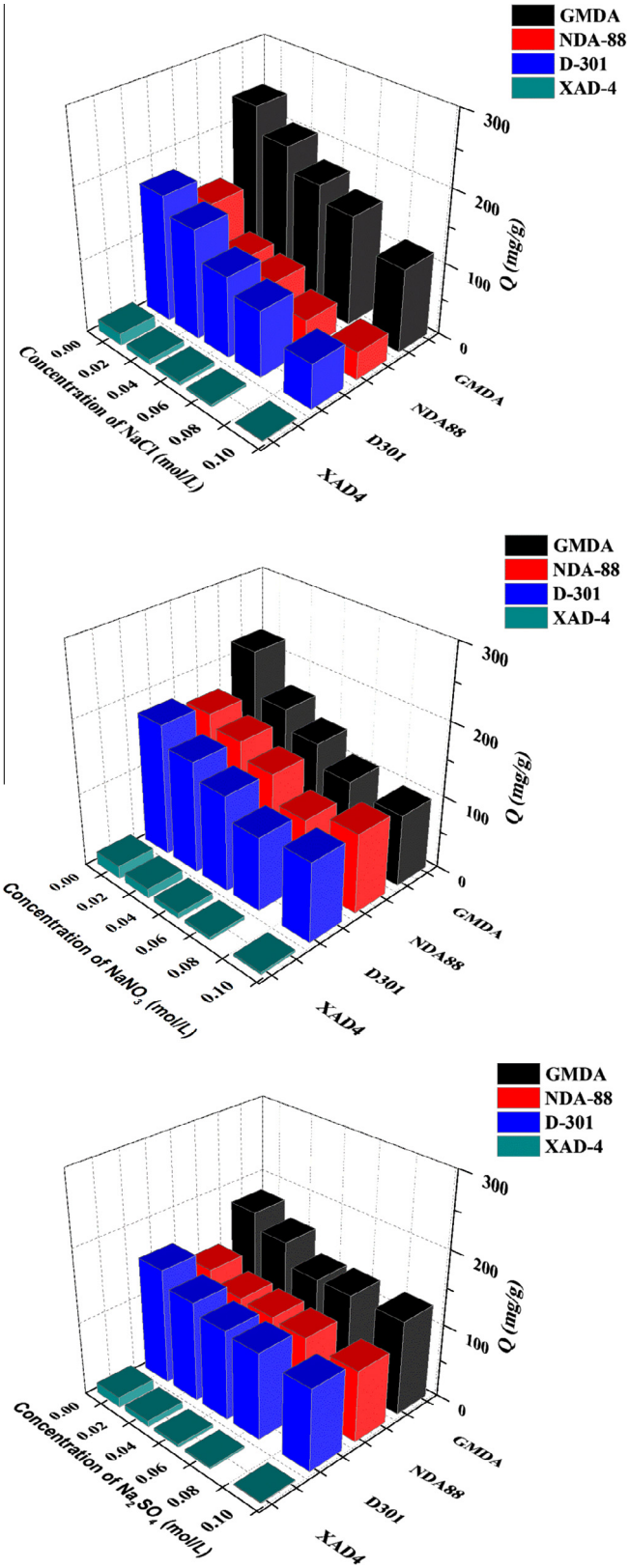

Fig. 8. The effect of coexisting ions Cl^-, NO_3^- and SO_4^{2-} on the removal of 200 mg/L H-acid by resins at 303 K. The concentrations of salt solution are 0.01, 0.03, 0.05, 0.07 and 0.1 M.

iment conditions. In order to further investigate the practicability of the GMDA resin, the regeneration experiments and column-mode experiment were conducted from the viewpoint of static adsorption and dynamic adsorption, respectively. The commercial resin NDA-88, D-301 and XAD-4 were used as the reference objects. After reaching the adsorption equilibrium, 0.05 g NDA-88 and D-301 resin were eluted by 0.5 mol/L NaOH solution [44,45]; 0.05 g XAD-4 resin was desorbed by 50% (v/v) ethanol aqueous solution [46]. Compared with the other three resins, GMDA occurs as quaternary amine groups in acidic environment. Nevertheless, amine functional groups were deprotonated in the strong basic environment. As a strong base, the sodium alkoxide (Na-OR) produced in the solution of ethanol and NaOH speeds up the process of deprotonation. An inspiration from the above desorption solvent was taken into account that different mixed desorption solvents can be used to desorb the H-acid molecular from the surface of the GMDA resin, and the ratio of desorption are shown in Table S2 in Supporting information. The results showed that the ratio of desorption of 4% (w/w) NaOH, 6% (w/w) NaCl and 50% (v/v) ethanol was higher than the others elution solvents. After desorption, the surface area of GMDA in Table S3 in Supporting information is close to the BET parameter of resin before adsorption. This shows that the experimental scheme is suitable for desorption of the GMDA resin.

Fig. 10 illustrates a 20 times-static regeneration adsorption cycles of H-acid onto four resins. As a common anion-exchange resin, D-301 resin maintains excellent performance on regeneration adsorption capacity in 20 times adsorption–desorption cycles, decreased from 288.10 to 146.10 mg/L. The resin GMDA exhibits a better property in regeneration with the adsorption amount after 3 times decreasing from 327.91 to 258.07 mg/L. Although some ups and downs of regenerative adsorption amount occur in the following 17 times, the curve maintains so stable trend that the practical application of GMDA resin can actually be an asset. On the contrary, for the hypercrosslinked resin NDA-88 with the mesopore and micropore, the adsorption capacity kept continuous and obvious decreasing from 220.93 to 106.30 mg/L. Moreover, because there were no functional groups on the exterior and interior surface, the adsorption amount of H-acid onto XAD-4 is minimum. The removal effect of H-acid molecular by the hydrophobic interaction is limited.

This adsorption equilibrium time is lower because of the wider pore structure and higher surface area than D-301 resin on the basis of the same functional groups [45,47]. This means the functional groups in the surface of GMDA resin can be fully desorbed by the desorption solvent. Unlike the matrix structure of D-301 resin, the regular and symmetrical amine functional groups of GMDA resin that widely spread on the surface can get the similar opportunities to be desorbed. Moreover, the high regeneration adsorption amount is a powerful proof of the anti-fouling performance of the novel adsorbent [18,47]. Wider pore diameter played an irreplaceable role in cycling process, and this characteristic reduced the possibility of pore occluded with the molecules of H-acid. The resin D-301 contains common functional group $N(CH_3)_2$ and its regeneration capacities kept reposefully which was not less than 200 mg/L, without obvious decrease after first desorption cycle. From the aspect of regeneration ability, the resin GMDA is deemed to be an ideal adsorbent to remove H-acid from the aqueous solution.

The complete system of a column experiment picked up with the four resins in the aqueous solution containing 1000 mg/L H-acid. The saturation adsorption ($C_t/C_0 > 98\%$) of H-acid onto GMDA, NDA-88, D-301 and XAD-4 was obtained at around 280, 176, 217 and 7 BV, respectively. Furthermore, as one of the most widely used models in column-mode experiment theory, Thomas model was used to calculate the maximum concentration of H-acid on resins, and the adsorption rate constant from the experiment data obtained in dynamic adsorption [48,49]. The fitted curves of dynamic adsorption are shown in Fig. 11. The expression of Thomas model is listed as follow:

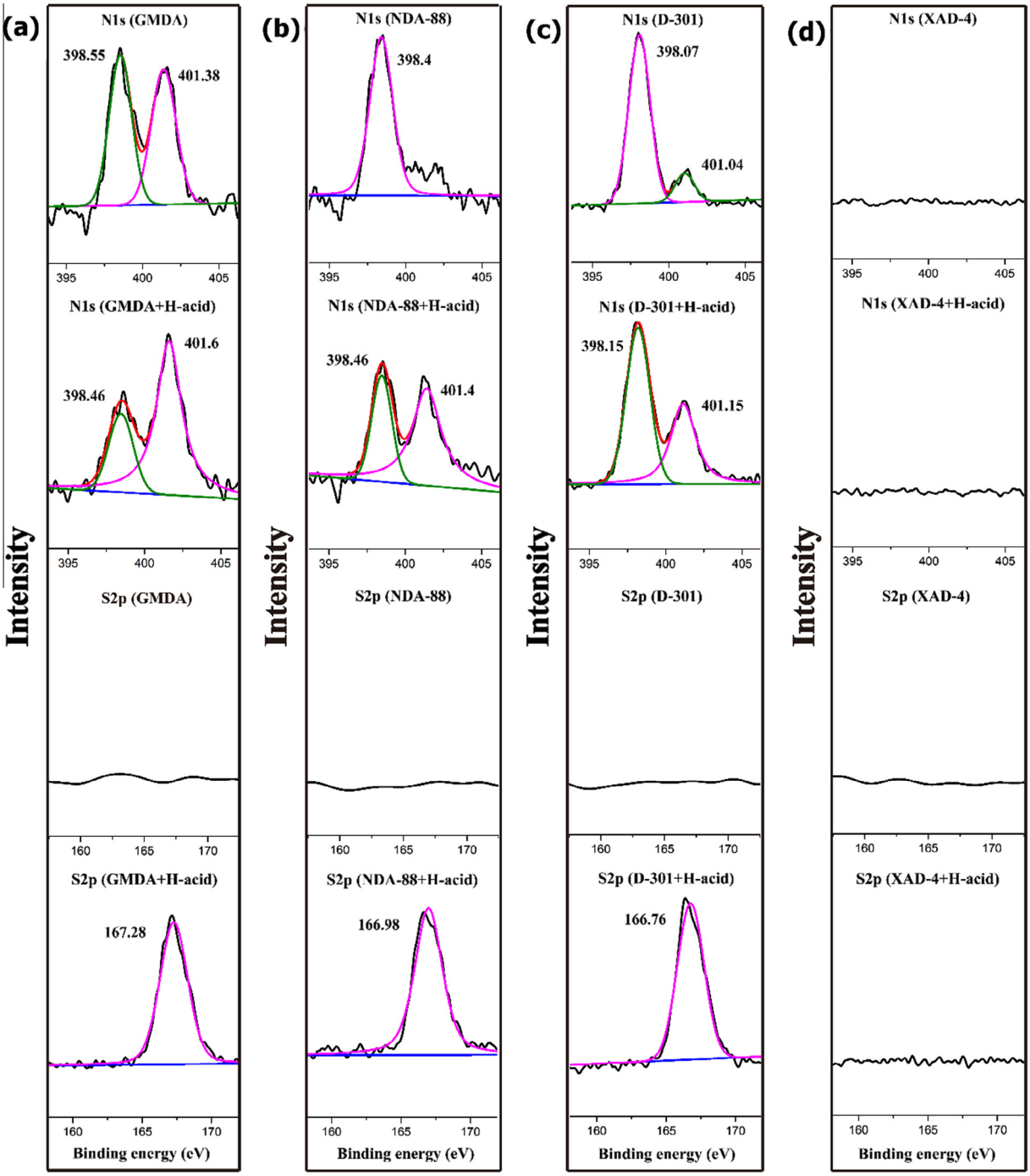

Fig. 9. XPS spectra of N1s and S2p of four resins before and after adsorption.

$$\frac{C_t}{C_0} = \frac{1}{1 + \exp(K_T/F(Q_T M - C_0 V N))} \quad (8)$$

where K_T (mL/(min * mg)) is Thomas rate constant, Q_T (mg/g) is the calculated theoretical saturate adsorption capacity by Thomas model, F (mL/min) is the flow rate of the H-acid solution, M (g) is the mass of resins, V (mL) is the effluent volume, C_0 (mg/L) is the concentration of H-acid solution, C_t (mg/L) is the H-acid solution concentration at time t and N is the bed volume number. The value of C_t/C_0 is the ratio of residual concentration at time t and initial H-acid concentrations, and the parameters were listed in Table 5. From the fitted data, the fitted curves of Thomas model fit the experiment data in a good form, and the four fitting degree R^2 are very close to 1. In addition, in the column adsorption, the theoretic adsorption capacities of H-acid onto resins are very close to their homologous experiment data. The aforementioned discussion indicated that the Thomas model is suitable to describe the adsorption of H-acid onto the four resins by the column experiment [50]. Moreover, although the same bed-volume weight of GMDA is heavier than that of three other resins, it's proved once again that the adsorption performance of GMDA is better than the others.

Consequently, the results of regeneration experiments and dynamic adsorption proved that the adsorption performance of H-acid onto the GMDA resin is the best among the four resins revealed in this work, both from an operational and an environmental viewpoint.

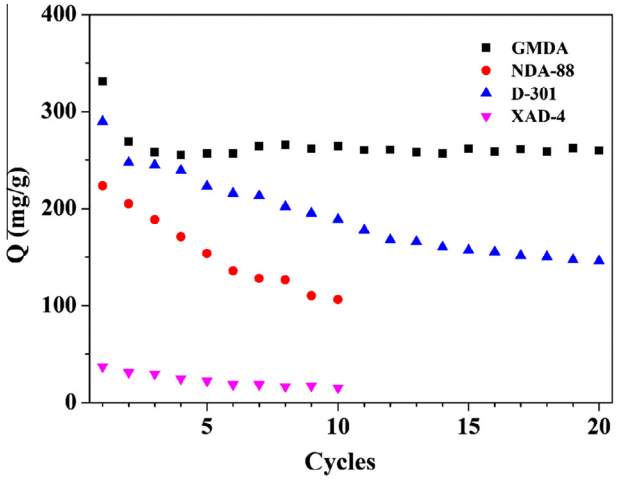

Fig. 10. The adsorption capacity of static regenerated resins at 303 K.

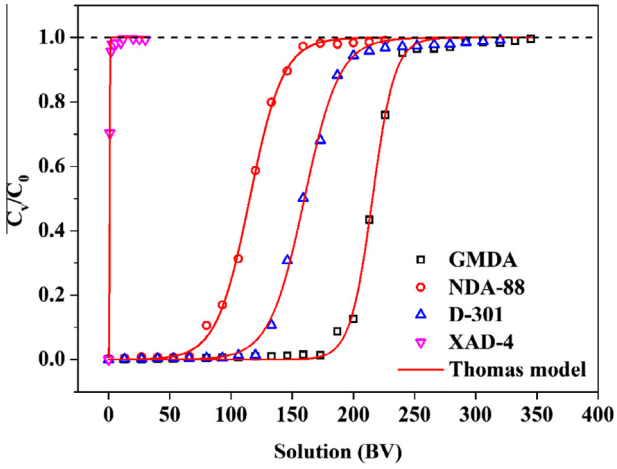

Fig. 11. The column-mode breakthrough curves of 1000 mg/L H-acid adsorption by GMDA, NDA-88, D-301 and XAD-4 at 303 K.

Table 5
Thomas model parameters of resins for the adsorption of H-acid in column systems at 303 K.

Resin	M (g)	K_T (mL/(min * mg))	Q_m (mg/g)	Q_T (mg/g)	R^2
GMDA	4.71	0.056	327.91	359.17	0.999
NDA-88	3.45	0.373	220.93	261.93	0.999
D-301	4.11	0.370	288.10	305.31	0.998
XAD-4	2.75	0.011	35.94	29.02	0.992

4. Conclusions

In the current work, a novel dimethylamine modified porous polymeric resin GMDA, containing the advantages of commercially available hypercrosslinked, anion-exchange and macroporous resins, is successfully synthesized. The resin GMDA brought the greater adsorption amount and rapid adsorption rate for H-acid than other three commercial resins (the hypercrosslinked NDA-88, the anion-exchange D-301 and the macroporous XAD-4), owing to its structural characteristics of wider pore diameter, higher selective functional amine groups and appropriate surface area. Zeta potential–pH profiles illustrate that no significant pH effect on the adsorption behaviors of H-acid onto the GMDA resin was observed in the pH range from 2 to 8, and electrostatic attraction is the major adsorption mechanism. The analysis of BET and SEM explain that the reasonable structure is the advantage source in adsorption process. From the FTIR and XPS, we can summarize a conclusion that H-acid molecule is adsorbed by resins very well. Finally, the new resin demonstrated desired regeneration capacity in adsorption–desorption cycles and better realistic adsorption performance in dynamic experiment. In summary, the resin GMDA can be considered an applicable adsorbent for the removal of H-acid. Meantime, the present study offers remarked guidance for not only further study of the adsorption behaviors of other naphthalene sulfonic acids onto polymeric resins, but also the structural design of resins according to the targeted contaminants.

Acknowledgments

This study was supported by the National Natural Science Foundation of China (Grant No. 51278253), the Project for Comprehensive Management of Tai Lake Water Environment in Jiangsu Province (TH2014206), the Natural Science Foundation of Jiangsu Province of China (BK20150981), the Natural Science Foundation of the Jiangsu Higher Education Institutions of China (15KJB610009), and Scientific Research Foundation for Advanced Talents of Nanjing Normal University (2014103XGQ0196). We also appreciate the Foundation of Jiangsu Collaborative Innovation Center of Biomedical Functional Materials and a project funded by the priority academic program development of Jiangsu Higher Education Institutions.

Appendix A. Supplementary data

Supplementary data associated with this article can be found, in the online version, at http://dx.doi.org/10.1016/j.cej.2015.08.010.

References

[1] K. Swaminathan, K. Pachhade, S. Sandhya, Decomposition of a dye intermediate, (H-acid) 1 amino-8-naphthol-3,6 disulfonic acid in aqueous solution by ozonation, Desalination 186 (2005) 155–164.
[2] Y. Zhang, X. Quan, S. Chen, Y. Zhao, F. Yang, Microwave assisted catalytic wet air oxidation of H-acid in aqueous solution under the atmospheric pressure using activated carbon as catalyst, J. Hazard. Mater. 137 (2006) 534–540.
[3] H. Liu, Q. Chen, Y. Yu, Z. Liu, G. Xue, Influence of Fenton's reagent doses on the degradation and mineralization of H-acid, J. Hazard. Mater. 263 (2013) 593–599.
[4] M. Noorjahan, M.P. Reddy, V.D. Kumari, B. Lavedrine, P. Boule, M. Subrahmanyam, Photocatalytic degradation of H-acid over a novel TiO_2 thin film fixed bed reactor and in aqueous suspensions, J. Photochem. Photobiol., A 156 (2003) 179–187.
[5] Z.C. Yuan, Y. Wang, X. Han, D.J. Chen, The adsorption behaviors of the multiple stimulus-responsive poly(ethylene glycol)-based hydrogels for removal of RhB dye, J. Appl. Polym. Sci. 132 (2015).
[6] I. Michael-Kordatou, C. Michael, X. Duan, X. He, D.D. Dionysiou, M.A. Mills, D. Fatta-Kassinos, Dissolved effluent organic matter: characteristics and potential implications in wastewater treatment and reuse applications, Water Res. 77 (2015) 213–248.
[7] P. Chularueangaksorn, S. Tanaka, S. Fujii, C. Kunacheva, Batch and column adsorption of perfluorooctane sulfonate on anion exchange resins and granular activated carbon, J. Appl. Polym. Sci. 131 (2014).
[8] M. Maretto, F. Bianchi, R. Vignola, S. Canepari, M. Baric, R. Iazzoni, M. Tagliabue, M.P. Papini, Microporous and mesoporous materials for the treatment of wastewater produced by petrochemical activities, J. Cleaner Prod. 77 (2014) 22–34.
[9] W.Q. Wang, J. Lv, J.M. Yang, S.N. Mei, Y.N. Li, H. Wan, Q.W. Yu, Application of extraction and adsorption to the alkylpyrazine removal from wastewater, Desalin. Water Treat. 54 (2015) 147–155.
[10] Z. Li, Y. Kong, Y. Ge, Synthesis of porous lignin xanthate resin for Pb^{2+} removal from aqueous solution, Chem. Eng. J. 270 (2015) 229–234.
[11] E. Guibal, T. Vincent, R. Navarro, Metal ion biosorption on chitosan for the synthesis of advanced materials, J. Mater. Sci. 49 (2014) 5505–5518.
[12] A. Yipmantin, H.J. Maldonado, M. Ly, J.M. Taulemesse, E. Guibal, Pb(II) and Cd (II) biosorption on *Chondracanthus chamissoi* (a red alga), J. Hazard. Mater. 185 (2011) 922–929.
[13] A.A. Galhoum, A.A. Atia, M.G. Mahfouz, S.T. Abdel-Rehem, N.A. Gomaa, T. Vincent, E. Guibal, Dy(III) recovery from dilute solutions using magnetic-

chitosan nano-based particles grafted with amino acids, J. Mater. Sci. 50 (2015) 2832–2848.
[14] W. Yang, F. Zheng, Y. Lu, X. Xue, N. Li, Adsorption interaction of tetracyclines with porous synthetic resins, Ind. Eng. Chem. Res. 50 (2011) 13892–13898.
[15] G. Xiao, L. Fu, A. Li, Enhanced adsorption of bisphenol A from water by acetylaniline modified hyper-cross-linked polymeric adsorbent: effect of the cross-linked bridge, Chem. Eng. J. 191 (2012) 171–176.
[16] W. Yang, X. Li, B. Pan, L. Lv, W. Zhang, Effective removal of effluent organic matter (EfOM) from bio-treated coking wastewater by a recyclable aminated hyper-cross-linked polymer, Water Res. 47 (2013) 4730–4738.
[17] W. Yang, Z. Yu, B. Pan, L. Lv, W. Zhang, Simultaneous organic/inorganic removal from water using a new nanocomposite adsorbent: a case study of *p*-nitrophenol and phosphate, Chem. Eng. J. 268 (2015) 399–407.
[18] Z. Lu, B. Jiang, A. Li, Investigation of the anti-fouling performance of an aminated resin, Chem. Eng. J. 193 (2012) 139–145.
[19] M.T. Gokmen, F.E. Du Prez, Porous polymer particles—a comprehensive guide to synthesis, characterization, functionalization and applications, Prog. Polym. Sci. 37 (2012) 365–405.
[20] J. Huang, X. Jin, J. Mao, B. Yuan, R. Deng, S. Deng, Synthesis, characterization and adsorption properties of diethylenetriamine-modified hypercrosslinked resins for efficient removal of salicylic acid from aqueous solution, J. Hazard. Mater. 217 (2012) 406–415.
[21] Z. Yuan, P. Yu, Y. Luo, Decolorisation of H-acid manufacturing process wastewater by anion exchange resin, Color. Technol. 123 (2007) 323–328.
[22] H.Y. Ding, J.F. Wang, J. Liu, Y.Z. Xu, R.Q. Chen, C.P. Wang, F.X. Chu, Preparation and properties of a novel flame retardant polyurethane quasi-prepolymer for toughening phenolic foam, J. Appl. Polym. Sci. 132 (2015).
[23] J. Wang, H. Li, C. Shuang, A. Li, C. Wang, Y. Huang, Effect of pore structure on adsorption behavior of ibuprofen by magnetic anion exchange resins, Microporous Mesoporous Mater. 210 (2015) 94–100.
[24] T. Nur, P. Loganathan, T.C. Nguyen, S. Vigneswaran, G. Singh, J. Kandasamy, Batch and column adsorption and desorption of fluoride using hydrous ferric oxide: solution chemistry and modeling, Chem. Eng. J. 247 (2014) 93–102.
[25] C. Shuang, P. Li, A. Li, Q. Zhou, M. Zhang, Y. Thou, Quaternized magnetic microspheres for the efficient removal of reactive dyes, Water Res. 46 (2012) 4417–4426.
[26] A.A. Galhoum, M.G. Mafhouz, S.T. Abdel-Rehem, N.A. Gomaa, A.A. Atia, T. Vincent, E. Guibal, Cysteine-functionalized chitosan magnetic nano-based particles for the recovery of light and heavy rare earth metals: uptake kinetics and sorption isotherms, Nanomaterials 5 (2015) 154–179.
[27] M.G. Mahfouz, A.A. Galhoum, N.A. Gomaa, S.S. Abdel-Rehem, A.A. Atia, T. Vincent, E. Guibal, Uranium extraction using magnetic nano-based particles of diethylenetriamine-functionalized chitosan: equilibrium and kinetic studies, Chem. Eng. J. 262 (2015) 198–209.
[28] L. Ji, W. Chen, L. Duan, D. Zhu, Mechanisms for strong adsorption of tetracycline to carbon nanotubes: a comparative study using activated carbon and graphite as adsorbents, Environ. Sci. Technol. 43 (2009) 2322–2327.
[29] D. Jia, C. Li, B. Zhao, S. Sun, Studies on the adsorption of 2-naphthalenesulfonic acid on basic resin from effluents, J. Chem. Eng. Data 55 (2010) 5801–5806.
[30] D. Jia, Y. Li, X. Shang, C. Li, Iron-impregnated weakly basic resin for the removal of 2-naphthalenesulfonic acid from aqueous solution, J. Chem. Eng. Data 56 (2011) 3881–3889.
[31] S. Deng, G. Zhang, X. Wang, T. Zheng, P. Wang, Preparation and performance of polyacrylonitrile fiber functionalized with iminodiacetic acid under microwave irradiation for adsorption of Cu(II) and Hg(II), Chem. Eng. J. 276 (2015) 349–357.
[32] D. Jermakowicz-Bartkowiak, P. Cyganowski, A. Lesniewicz, W. Tylus, J. Checmanowski, A. Marcinowska, Spontaneous formation of gold microplates during reduction-coupled removal of noble metals using Dowex M4195 resin, J. Appl. Polym. Sci. 132 (2015).
[33] L. Ding, H. Deng, C. Wu, X. Han, Affecting factors, equilibrium, kinetics and thermodynamics of bromide removal from aqueous solutions by MIEX resin, Chem. Eng. J. 181 (2012) 360–370.
[34] P. Rudnicki, Z. Hubicki, D. Kolodynska, Evaluation of heavy metal ions removal from acidic waste water streams, Chem. Eng. J. 252 (2014) 362–373.
[35] Y. Zhan, J. Lin, Z. Zhu, Removal of nitrate from aqueous solution using cetylpyridinium bromide (CPB) modified zeolite as adsorbent, J. Hazard. Mater. 186 (2011) 1972–1978.
[36] X. Xu, B. Gao, Q. Yue, Q. Li, Y. Wang, Nitrate adsorption by multiple biomaterial based resins: application of pilot-scale and lab-scale products, Chem. Eng. J. 234 (2013) 397–405.
[37] M.S.-L. Yee, P.S. Khiew, Y.F. Tan, Y.-Y. Kok, K.W. Cheong, W.S. Chiu, C.-O. Leong, Potent antifouling silver-polymer nanocomposite microspheres using ion-exchange resin as templating matrix, Colloids Surf., A 457 (2014) 382–391.
[38] X. Xing, B.-Y. Gao, Q.-Q. Zhong, Q.-Y. Yue, Q. Li, Sorption of nitrate onto amine-crosslinked wheat straw: characteristics, column sorption and desorption properties, J. Hazard. Mater. 186 (2011) 206–211.
[39] N. Ates, F.B. Incetan, Competition impact of sulfate on NOM removal by anion-exchange resins in high-sulfate and low-SUVA waters, Ind. Eng. Chem. Res. 52 (2013) 14261–14269.
[40] J. Huang, L. Yang, X. Wu, M. Xu, Y.-N. Liu, S. Deng, Phenol adsorption on alpha, alpha′-dichloro-*p*-xylene (DCX) and 4,4′-bis(chloromethyl)-1,1′-hiphenyl (BCMBP) modified XAD-4 resins from aqueous solutions, Chem. Eng. J. 222 (2013) 1–8.
[41] L. Cui, Y. Wang, L. Gao, L. Hu, Q. Wei, B. Du, Removal of Hg(II) from aqueous solution by resin loaded magnetic beta-cyclodextrin bead and graphene oxide sheet: synthesis, adsorption mechanism and separation properties, J. Colloid Interface Sci. 456 (2015) 42–49.
[42] J. Chen, Z.S. Liu, K. Li, J.R. Huang, X.A. Nie, Y.H. Zhou, Synthesis and application of a natural plasticizer based on cardanol for poly(vinyl chloride), J. Appl. Polym. Sci. 132 (2015).
[43] G. Lawrie, I. Keen, B. Drew, A. Chandler-Temple, L. Rintoul, P. Fredericks, L. Grondahl, Interactions between alginate and chitosan biopolymers characterized using FTIR and XPS, Biomacromolecules 8 (2007) 2533–2541.
[44] G.Q. Xiao, L.P. Long, J.L. Wang, Synthesis of the water-compatible *p*-acetaminophen resin and its adsorption performances for vanillin in aqueous solution, Chin. Chem. Lett. 23 (2012) 123–126.
[45] B.C. Pan, Q.X. Zhang, F.W. Meng, X.T. Li, X. Zhang, J.Z. Zheng, W.M. Zhang, B.J. Pan, J.L. Chen, Sorption enhancement of aromatic Sulfonates onto an aminated hyper-cross-linked polymer, Environ. Sci. Technol. 39 (2005) 3308–3313.
[46] C.Y. Li, M.W. Xu, X.C. Sun, S. Han, X.F. Wu, Y.N. Liu, J.H. Huang, S.G. Deng, Chemical modification of Amberlite XAD-4 by carbonyl groups for phenol adsorption from wastewater, Chem. Eng. J. 229 (2013) 20–26.
[47] B.C. Pan, J.S. Xu, B. Wu, Z.G. Li, X.T. Liu, Enhanced removal of fluoride by polystyrene anion exchanger supported hydrous zirconium oxide nanoparticles, Environ. Sci. Technol. 47 (2013) 9347–9354.
[48] X. Zhang, T.N. Brown, A. Ansari, B. Yeun, K. Kitaoka, A. Kondo, Y.D. Lei, F. Wania, Effect of wind on the chemical uptake kinetics of a passive air sampler, Environ. Sci. Technol. 47 (2013) 7868–7875.
[49] T. Chen, F. Liu, C. Ling, J. Gao, C. Xu, L. Li, A. Li, Insight into highly efficient coremoval of copper and *p*-nitrophenol by a newly synthesized polyamine chelating resin from aqueous media: competition and enhancement effect upon site recognition, Environ. Sci. Technol. 47 (2013) 13652–13660.
[50] W. Zhang, H. Yan, H. Li, Z. Jiang, L. Dong, X. Kan, H. Yang, A. Li, R. Cheng, Removal of dyes from aqueous solutions by straw based adsorbents: batch and column studies, Chem. Eng. J. 168 (2011) 1120–1127.